GEOPHYSICAL RESEARCH LETTERS, VOL. 34, L20401, doi:10.1029/2007GL031088, 2007

Initial soil moisture retrievals from the METOP-A Advanced Scatterometer (ASCAT)

Zoltan Bartalis,[1] Wolfgang Wagner,[1] Vahid Naeimi,[1] Stefan Hasenauer,[1] Klaus Scipal,[2] Hans Bonekamp,[3] Julia Figa,[3] and Craig Anderson[3]

Received 22 June 2007; revised 31 July 2007; accepted 11 September 2007; published 16 October 2007.

[1] This article presents first results of deriving relative surface soil moisture from the METOP-A Advanced Scatterometer. Retrieval is based on a change detection approach which has originally been developed for the Active Microwave Instrument flown onboard the European satellites ERS-1 and ERS-2. Using model parameters derived from eight years of ERS scatterometer data, first global soil moisture maps have been produced from ASCAT data. The ASCAT data were distributed by EUMETSAT for validation purposes during the ASCAT product commissioning activities. Several recent cases of drought and excessive rainfall are clearly visible in the soil moisture data. The results confirm that seamless soil moisture time series can be expected from the series of two ERS and three METOP scatterometers, providing global coverage on decadal time scales (from 1991 to about 2021). Thereby, operational, near-real-time ASCAT soil moisture products will become available for weather prediction and hydrometeorological applications. **Citation:** Bartalis, Z., W. Wagner, V. Naeimi, S. Hasenauer, K. Scipal, H. Bonekamp, J. Figa, and C. Anderson (2007), Initial soil moisture retrievals from the METOP-A Advanced Scatterometer (ASCAT), *Geophys. Res. Lett.*, *34*, L20401, doi:10.1029/2007GL031088.

1. Introduction

[2] The primary objective of spaceborne scatterometers (real aperture radar instruments) is wind retrieval over oceans [*Stoffelen*, 1998]. When they operate over land, the backscattered signal being measured contains substantial information about soil moisture, among others [*Ulaby et al.*, 1982]. Several authors have proposed methods for retrieving soil moisture from coarse-resolution (50 km) scatterometer data as provided by the European satellites ERS-1 and ERS-2 [*Magagi and Kerr*, 2001; *Pulliainen et al.*, 1998; *Wen and Su*, 2003; *Woodhouse and Hoekman*, 2000; *Zine et al.*, 2005]. Using the change detection approach suggested by *Wagner et al.* [1999], the first global, multi-year soil moisture data set was derived by *Scipal* [2002]. Various studies showed that this data set reflects trends in precipitation [*Fontaine et al.*, 2007; *Wagner et al.*, 2003], modeled soil moisture [*Dirmeyer et al.*, 2004; *Pellarin et al.*, 2006], in situ soil moisture observations [*Ceballos et al.*, 2005], and runoff [*Scipal et al.*, 2005]. The dataset is also complementary to the series of GRACE gravitational observations related to the dynamics of the continental water storage [*Wahr et al.*, 2004].

[3] With the recent launch of the first of three METOP satellites in October 2006, the Advanced Scatterometer (ASCAT) instrument takes over and enhances the role of the ERS scatterometers by adding the operational aspect of the service [*Klaes et al.*, 2007]. Despite changes in the design and the availability of a second swath, ASCAT is similar to the ERS scatterometer [e.g., *Gelsthorpe et al.*, 2000]. Therefore, soil moisture algorithms developed for the ERS scatterometer are expected to be directly transferable to ASCAT, requiring only minor adaptations of the processing chain and configuration. Hence, using ASCAT commissioning data, a first test of the applicability of the soil moisture retrieval method proposed by *Wagner et al.* [1999] could be performed. In this paper, the retrieval method is shortly described, followed by some first examples of composite images of ASCAT-based soil moisture and its anomaly compared to corresponding images of precipitation or NDVI anomalies, thereby confirming some recent cases of extreme rain events or droughts.

2. Scatterometers and Soil Moisture

[4] Both the ERS scatterometer and ASCAT are real-aperture radar instruments, measuring surface radar backscatter with very good radiometric accuracy and stability. They produce backscatter measurements with a spatial resolution of circa 50 km and a good radiometric resolution [*Figa-Saldaña et al.*, 2002], using VV polarization in the C-band (5.255 GHz).

[5] ASCAT transmits linear frequency-modulated pulses (“chirp”) with a markedly longer duration of around 10 ms at a relatively low peak power of 120 W [*Gelsthorpe et al.*, 2000]. ASCAT measures on both sides of the subsatellite track, producing two swaths of data. This double swath and the fact that it operates continuously, give more than twice the coverage (almost daily) of that provided by the ERS scatterometers. For each pass above an observed location within the swath(s), both the ASCAT and ERS scatterometers produce a triplet of σ^0 backscattering coefficients, from the three different antenna beams. A σ^0 measurement is the result of averaging several radar echoes, which in the case of 50 km resolution products is resampled to a 25 km grid in the swath geometry. A similar higher resolution product (circa 30 km) is produced from ASCAT, in this case on a 12.5 km swath grid.

[1] Institute of Photogrammetry and Remote Sensing, Vienna University of Technology, Vienna, Austria.

[2] European Centre for Medium-Range Weather Forecasts (ECMWF), Reading, U. K.

[3] European Organisation for the Exploitation of Meteorological Satellites (EUMETSAT), Darmstadt, Germany.

0094-8276/07/2007GL031088$05.00

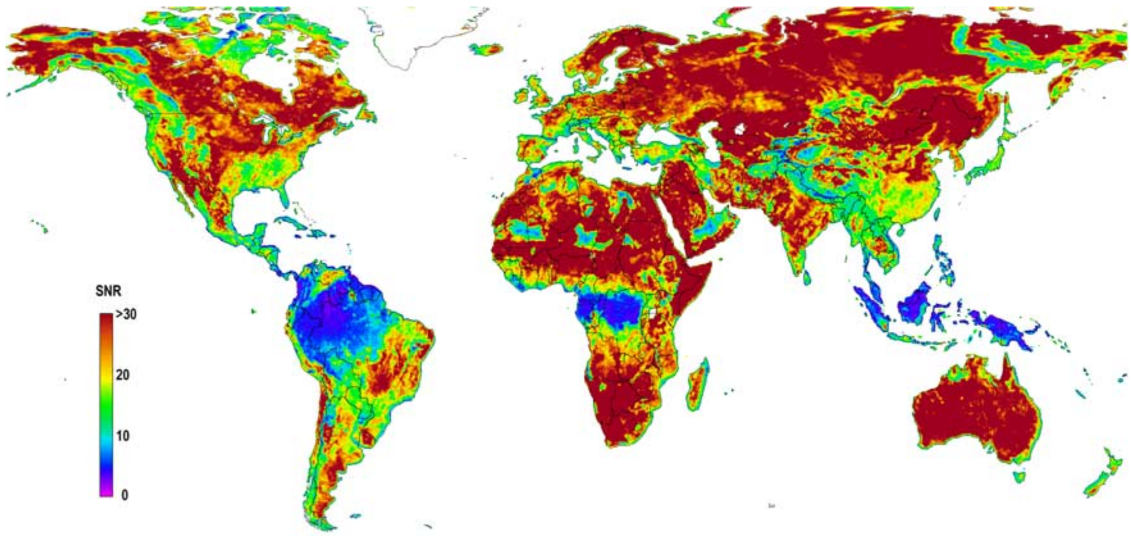

Figure 1. Map illustrating the performance of the soil moisture retrieval method. The signal-to-noise ratio (SNR) is defined as the ratio between the sensitivity to soil moisture (the difference between wet and dry reference values) and the yearly mean noise of σ^0 normalized to 40° incidence angle.

[6] Due to the antenna design, the three (fore, mid and aft beam) measurements are made at a 45°, 90° and 135° azimuth angle with respect to the satellite track (on each side in the case of ASCAT). The fore and aft beam measurements are made under equal incidence angle ranges, while the mid-beam measurements have slightly lower incidence angle range. The ability to register backscatter at various incidence angles makes it possible to determine the yearly cycle of the backscatter-incidence angle relationship, an essential prerequisite for correcting seasonal vegetation effects. Although current understanding of the theoretical aspects of the attenuation of microwaves by vegetation is rather poor, various experimental studies [e.g., *Brown et al.*, 2003; *Pulliainen et al.*, 1998] have shown the presence of significant soil response at C-band frequencies even in the case of vegetated areas, especially when observed at lower incidence angles. Using a time series-based change detection approach for soil moisture retrieval also proves beneficial in minimizing the vegetation influence. Once the backscatter is normalized to a standard incidence angle (40°), its further variations are considered to be either vegetation-induced, due to soil moisture or noise. Soil moisture is considered to have a linear relationship to backscatter in the decibel space, while the noise sources include the instrument noise, speckle and azimuthal anisotropies. The surface roughness is assumed to have a constant contribution in time, and therefore is not accounted for in the change detection algorithm. By knowing the typical yearly vegetation cycle and how it influences the backscatter-incidence angle relationship for each location on the Earth, the vegetation effects can be removed, revealing the soil moisture variations. As a last step, the historically lowest and highest values of observed soil moisture are assigned to the 0% (dry) and 100% (wet) references respectively, thereby yielding time series of relative soil moisture percentage values for the first few centimeters of the soil. These values can be converted to absolute soil moisture using soil properties [*Wagner et al.*, 1999] or to profile soil moisture values by using information inherent in the antecedent values of the same time series [*Ceballos et al.*, 2005]. A complete characterization of the error propagation is also done in the course of the different algorithm steps.

[7] Figure 1 illustrates the global performance of the method by using a signal-to-noise ratio (SNR) index. This relative index represents the ratio of sensitivity to soil moisture (measured as the difference between the wet and dry references) and the mean noise of backscatter coefficient σ^0 normalized to a 40° incidence angle. High SNR characterizes areas particularly suitable for soil moisture retrieval (grasslands, savannas, tundra, agricultural land, etc.). In spite of high SNR values, special care has to be taken when working with boreal areas, where the soil moisture information might suffer from the influence of forest canopies, ground frost and snow, water content of the moss and peat substrata rather than the soil itself, etc.

[8] A low SNR is typically displayed by rainforests, where the radar signal does not penetrate the dense vegetation [*Long and Skouson*, 1996]. In such areas the sensitivity to soil moisture is thus too small. Other low SNR areas display high azimuthal anisotropy and/or volume scattering, such as sand deserts (with aligned dunes and ripples), large urban areas and other regions of complex topography [*Bartalis et al.*, 2006]. In these cases, the sensitivity to soil moisture might be very large (deserts), but the noise induced by azimuthal effects and volume scattering has a stronger influence and the final SNR will be small. Summarizing Figure 1, retrieval of soil moisture is made impossible in areas where the SNR is less than 10 and should be used carefully in areas where SNR < 20.

3. Examples of Soil Moisture Extremes

[9] For the work presented in this paper, we have used March 2007 data that was made available during the commissioning phase of the ASCAT instrument with retrieval model parameters (related to vegetation correction, the wet and dry reference, etc.) derived from historical ERS

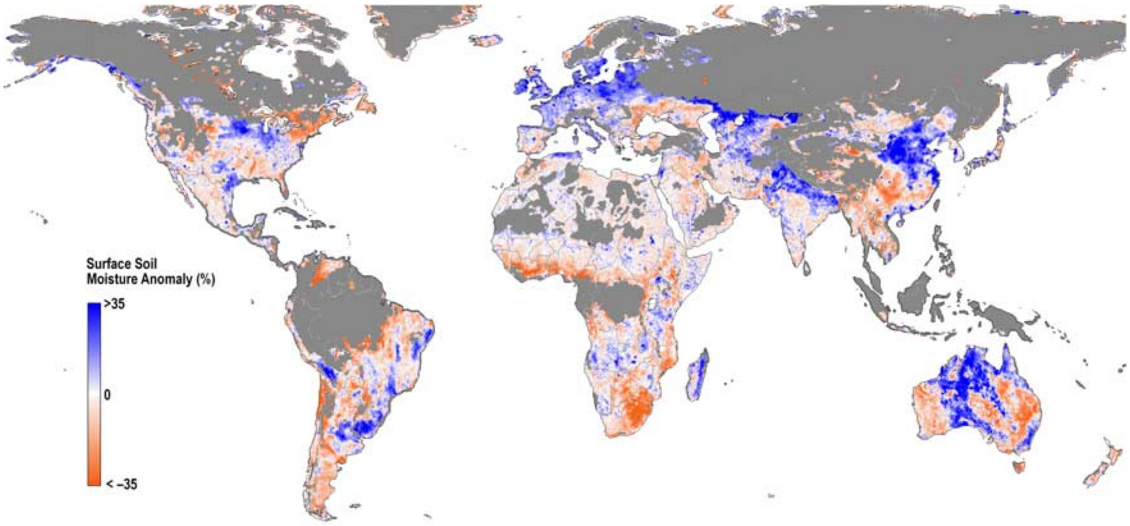

Figure 2. Surface soil moisture anomaly situation for the period 15–21 March 2007. Blue areas are wetter than the 1992–2000 average for that period of the year, while red areas are dryer. Areas where no soil moisture can be retrieved or where soil moisture is meaningless (according to a snow cover climatology for the period) are masked out.

data from 1992–2000. The resulting ASCAT soil moisture data sets are "first looks' data and may change since the instrument calibration-validation has yet to be finalized, including possible cross-calibration between ASCAT and ERS data. Improved calibration coefficients for ASCAT are expected later into the commissioning, when the complete data set is planned to be reprocessed accordingly. The overlap in time between the operation of ASCAT and the ERS-2 scatterometer will also allow for better evaluation of possible biases between the instruments.

[10] Figure 2 shows the situation of the surface soil moisture anomaly (compared to the 1992–2000 mean from ERS) for a seven day period in spring 2007 (15–21 March). Areas where the retrieval method cannot deliver soil moisture information (tropical forests, sand deserts, etc.) have been masked out. Also masked out are areas where the probability of snow cover exceeds 50% for the considered period, based on a historic analysis of SSM/I snow cover data [*Nolin et al.*, 1998]. Wetter conditions than normal are observed in northeastern China, due to the heavy precipitation over the North China Plain recorded a week earlier, as reported by the United States Department of Agriculture (USDA) Foreign Agricultural Service (FAS) (http://www.pecad.fas.usda.gov). The winter drought conditions reported in the Chinese southeastern provinces of Guizhou and Sichuan (source: Xinhua news agency), a result of several months long lack of rainfall, are also confirmed in the image.

[11] A closer look at the snow-free southern hemisphere reveals more clearly delimited areas of rain events or droughts. The extremely wet conditions in northeastern Argentina and Uruguay correspond to one of the worst

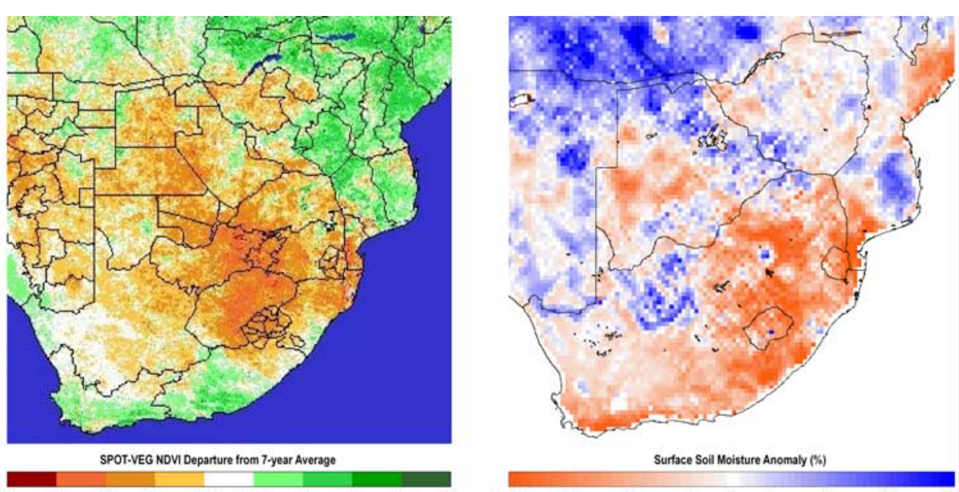

Figure 3. Comparison between (left) SPOT Vegetation NDVI (Normalized Difference of Vegetation Index) departure from 7-year average (source: USDA Foreign Agricultural Service, http://www.pecad.fas.usda.gov/cropexplorer) and (right) ASCAT-derived surface soil moisture anomaly for the period 21–31 March 2007.

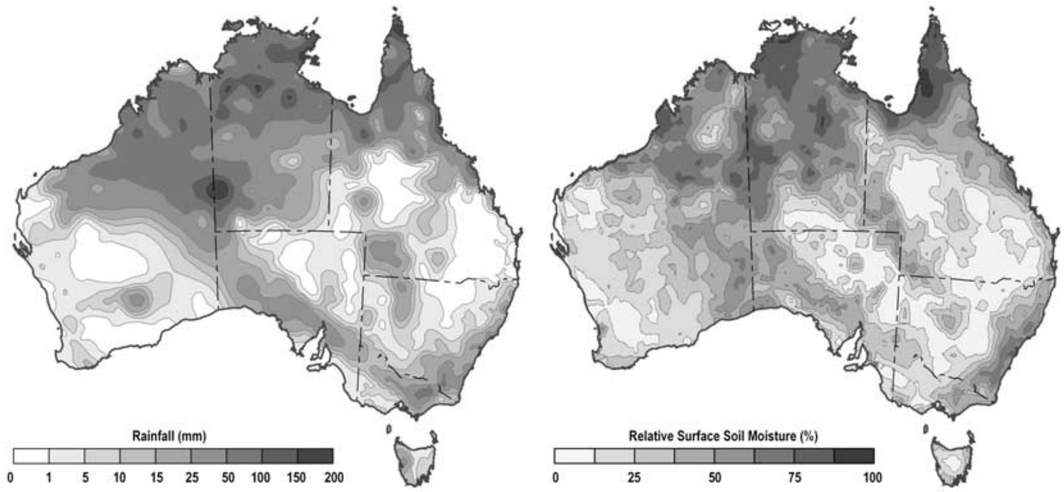

Figure 4. (left) Interpolated in situ rainfall (source: Australian Government, Bureau of Meteorology, http://www.bom.gov.au/climate) and (right) ASCAT-derived relative surface soil moisture comparison for Australia during 15–21 March 2007.

rainy periods in the last hundred years in this region, with thousands of evacuations and almost two thirds of the farmland devastated by mid-April (source: Financial Times Information Limited).

[12] Also in Figure 2, severe drought is visible in southern Africa, notably in the eastern half of South Africa. Almost record-high temperatures and lack of precipitation from January through March caused serious crop damage and deficiency in crop planting, as reported by USDA FAS. This situation is also clearly shown in Figure 3, where SPOT Vegetation-derived NDVI (Normalized Difference of Vegetation Index) anomaly is compared to the ASCAT surface soil moisture anomaly for the period 21–31 March 2007. The overall patterns compare well, despite some local discrepancies, partly due to the fact that NDVI anomalies are based on long-term averages over the last seven years while the soil moisture anomalies use 1992–2000 as a reference. Also, NDVI does not react quickly enough to short-term soil moisture variations, which could explain some of the discrepancies in the upper part of the images. The strikingly unusual soil moisture conditions over Australia in Figure 2 are shown in detail in Figure 4 where the ASCAT relative surface soil moisture (rather than its anomaly) is compared to interpolated in situ rainfall measurements provided by the Australian Bureau of Meteorology. The month of March 2007 was particularly wet all over the Australian continent, with total precipitation reaching 45% above normal amounts. For the depicted week, three tropical cyclones (George, Jacob and Kara) were responsible for the high rainfall over the central-northern parts of Western Australia and the Northern Territory. The wet area extending as a strip across Southern Australia, visible in both the rainfall and the soil moisture images, as well as the relatively dry conditions over parts of Queensland were another feature of the month of March as a whole. When surface soil moisture images of successive overpasses were considered (not shown here), the rainfall related to the three above-mentioned tropical cyclones could be easily tracked as the cyclones advanced inland from their landfall points. Also, increase in wetness due to smaller-scale rain events especially over the arid central Australian regions could be sharply distinguished.

4. Conclusion

[13] A first look at surface soil moisture products derived from ASCAT data in combination with the ERS long-term scattering parameter database show promising results in observing both extreme wetness and drought. The presented snapshot and comparisons between the ASCAT relative surface soil moisture and the corresponding situation of the rainfall and NDVI proxies are intended as a visual exercise only. Any in-depth validation would have to closely consider the overall spatial and temporal variability of hydrological processes such as rainfall, vegetation and water runoff and storage. Nevertheless, the exposed case studies illustrate well the potential of the ASCAT instrument to monitor soil moisture with an almost daily temporal sampling at a spatial resolution of 50 km or better. After the ASCAT commissioning, conditions will be met for continuing the global, long-term (30 years) soil moisture time series, which the ERS-1 scatterometer initiated in 1991. Operational dissemination of the ASCAT Level 2 soil moisture product by EUMETSAT is foreseen, with processing algorithms and software developed in cooperation with Vienna University of Technology (TU Wien). This service is envisaged to start operations in 2008, and will provide surface soil moisture estimations on a 25 km grid in the ASCAT swath, within 135 minutes of data acquisition and with global coverage. Given the limitations and caveats of both active and passive microwave remote sensing of soil moisture [*Kerr*, 2007; *Wagner et al.*, 2007], it is expected that the ASCAT soil moisture service will mutually benefit soil moisture observations provided by the Soil Moisture and Ocean Salinity (SMOS) mission [*Kerr et al.*, 2001] and other passive microwave instruments [*Njoku et al.*, 2003], becoming useful for hydrology, agrometeorology, weather prediction, climate research and other applications.

[14] **Acknowledgments.** This work has been supported by the Austrian Science Fund (L148-N10), EUMETSAT (EUM/CO/05/1421/HGB, H-SAF, NWP SAF Associate Scientist Programme), and the European Commission (geoland).

References

Bartalis, Z., et al. (2006), Azimuthal anisotropy of scatterometer measurements over land, *IEEE Trans. Geosci. Remote Sens.*, *44*, 2083–2092.

Brown, S. C. M., et al. (2003), High-resolution measurements of scattering in wheat canopies: Implications for crop parameter retrieval, *IEEE Trans. Geosci. Remote Sens.*, *41*, 1602–1610.

Ceballos, A., et al. (2005), Validation of ERS scatterometer-derived soil moisture data in the central part of the Duero Basin, Spain, *Hydrol. Processes*, *19*, 1549–1566.

Dirmeyer, P. A., et al. (2004), Comparison, validation, and transferability of eight multiyear global soil wetness products, *J. Hydrometeorol.*, *5*, 1011–1033.

Figa-Saldaña, J., et al. (2002), The advanced scatterometer (ASCAT) on the meteorological operational (MetOp) platform: A follow on for European wind scatterometers, *Can. J. Remote Sens.*, *28*, 404–412.

Fontaine, B., et al. (2007), Fluctuations in annual cycles and inter-seasonal memory in West Africa: Rainfall, soil moisture and heat fluxes, *Theor. Appl. Climatol.*, *88*, 57–70.

Gelsthorpe, R. V., et al. (2000), ASCAT—Metop's advanced scatterometer, *ESA Bull.*, *102*, 19–27.

Kerr, Y. H. (2007), Soil moisture from space: Where are we?, *Hydrogeol. J.*, *15*, 117–120.

Kerr, Y. H., et al. (2001), Soil moisture retrieval from space: The Soil Moisture and Ocean Salinity (SMOS) mission, *IEEE Trans. Geosci. Remote Sens.*, *39*, 1729–1735.

Klaes, D., et al. (2007), An introduction to the EUMETSAT Polar System, *Bull. Am. Meteorol. Soc.*, *88*, 1085–1096, doi:10.1175/BAMS-88-7-1085.

Long, D. G., and G. B. Skouson (1996), Calibration of spaceborne scatterometers using tropical rain forests, *IEEE Trans. Geosci. Remote Sens.*, *34*, 413–424.

Magagi, R. D., and Y. H. Kerr (2001), Estimating surface soil moisture and soil roughness over semiarid areas from the use of the copolarization ratio, *Remote Sens. Environ*, *75*, 432–445.

Njoku, E. G., et al. (2003), Soil moisture retrieval from AMSR-E, *IEEE Trans. Geosci. Remote Sens.*, *41*, 215–229.

Nolin, A., R. L. Armstrong, and J. Maslanik (1998), Near real-time SSM/I EASE-grid daily global ice concentration and snow extent, http://nsidc.org/data/nise1.html, Natl. Snow and Ice Data Cent., Boulder, Colo.

Pellarin, T., et al. (2006), Evaluation of ERS scatterometer soil moisture products over a half-degree region in southwestern France, *Geophys. Res. Lett.*, *33*, L17401, doi:10.1029/2006GL027231.

Pulliainen, J. T., et al. (1998), Application of ERS-1 wind scatterometer data to soil frost and soil moisture monitoring in boreal forest zone, *IEEE Trans. Geosci. Remote Sens.*, *36*, 849–863.

Scipal, K. (2002), Global soil moisture retrieval from ERS scatterometer data, Ph.D. diss., Vienna Univ. of Technol., Vienna, Austria.

Scipal, K., et al. (2005), Soil moisture-runoff relation at the catchment scale as observed with coarse resolution microwave remote sensing, *Hydrol. Earth Syst. Sci.*, *9*, 173–183.

Stoffelen, A. (1998), Scatterometry, Ph.D. diss., Utrecht Univ., Utrecht, Netherlands.

Ulaby, F. T., et al. (1982), *Microwave Remote Sensing: Active and Passive*, vol. 2, *Radar Remote Sensing and Surface Scattering and Emission Theory*, 609 pp., Addison-Wesley, Reading, Mass.

Wagner, W., et al. (1999), A method for estimating soil moisture from ERS scatterometer and soil data, *Remote Sens. Environ.*, *70*, 191–207.

Wagner, W., K. Scipal, C. Pathe, D. Gerten, W. Lucht, and B. Rudolf (2003), Evaluation of the agreement between the first global remotely sensed soil moisture data with model and precipitation data, *J. Geophys. Res.*, *108*(D19), 4611, doi:10.1029/2003JD003663.

Wagner, W., et al. (2007), Operational readiness of microwave remote sensing of soil moisture for hydrologic applications, *Nord. Hydrol.*, *38*, 1–20.

Wahr, J., et al. (2004), Time-variable gravity from GRACE: First results, *Geophys. Res. Lett.*, *31*, L11501, doi:10.1029/2004GL019779.

Wen, J., and Z. Su (2003), A time series based method for estimating relative soil moisture with ERS wind scatterometer data, *Geophys. Res. Lett.*, *30*(7), 1397, doi:10.1029/2002GL016557.

Woodhouse, I. H., and D. H. Hoekman (2000), A model-based determination of soil moisture trends in Spain with the ERS-scatterometer, *IEEE Trans. Geosci. Remote Sens.*, *38*, 1783–1793.

Zine, S., et al. (2005), Land surface parameter monitoring with ERS scatterometer data over the Sahel: A comparison between agro-pastoral and pastoral areas, *Remote Sens Environ.*, *96*, 438–452.

C. Anderson, H. Bonekamp, and J. Figa, European Organisation for the Exploitation of Meteorological Satellites (EUMETSAT), Am Kavalleriesand 31, D-64295 Darmstadt, Germany.

Z. Bartalis, S. Hasenauer, V. Naeimi, and W. Wagner, Institute of Photogrammetry and Remote Sensing, Vienna University of Technology, Gusshausstrasse 27-29/E122, A-1040 Wien, Austria. (zb@ipf.tuwien.ac.at)

K. Scipal, European Centre for Medium-Range Weather Forecasts (ECMWF), Shinfield Park, Reading RG2 9AX, UK.